

# Thermal fracture as a framework for crack propagation law

F. Corson<sup>†</sup>, M. Adda-Bedia<sup>†</sup>, H. Henry<sup>‡</sup> and E. Katzav<sup>†</sup>

<sup>†</sup>Laboratoire de Physique Statistique de l'Ecole Normale Supérieure, CNRS UMR 8550,  
24 rue Lhomond, 75231 Paris Cedex 05, France.

<sup>‡</sup>Laboratoire de Physique de la Matière condensée, CNRS UMR 7643,  
Ecole Polytechnique, 91128 Palaiseau Cedex, France.

October 24, 2018

## Abstract

We address analytically and numerically the problem of crack path prediction in the model system of a crack propagating under thermal loading. We show that one can explain the instability from a straight to a wavy crack propagation by using only the principle of local symmetry and the Griffith criterion. We then argue that the calculations of the stress intensity factors can be combined with the standard crack propagation criteria to obtain the evolution equation for the crack tip within any loading configuration. The theoretical results of the thermal crack problem agree with the numerical simulations we performed using a phase field model. Moreover, it turns out that the phase-field model allows to clarify the nature of the transition between straight and oscillatory cracks which is shown to be supercritical. We also show that this numerical approach is superior to the classical methods of crack path prediction and it would be especially suitable when considering complex moving crack fronts.

## 1 Introduction

Crack path prediction is one of the main challenges in the field of fracture mechanics. The reason is simple - a satisfactory equation of motion of a crack tip is associated with a fundamental understanding of material separation mechanisms (Freund, 1990; Broberg, 1999; Fineberg and Marder, 1999; Adda-Bedia et al., 1999; Leblond, 2003). From a more general point of view and alongside its importance in many applications, the determination of crack propagation laws is necessary to describe the fracture phenomenon as a pattern formation process induced by mechanical stresses. Within the framework of Linear Elastic Fracture Mechanics (LEFM), the propagation of a crack is mainly governed by the singular behavior of the stress field in the vicinity of its tip (Freund, 1990; Broberg, 1999; Leblond, 2003). For a two-dimensional quasi-static crack, which is the main purpose of the present work, this behavior is given by

$$\sigma_{ij}(r, \phi) = \frac{K_I}{\sqrt{2\pi r}} \Sigma_{ij}^I(\phi) + \frac{K_{II}}{\sqrt{2\pi r}} \Sigma_{ij}^{II}(\phi) + O(r^0), \quad (1)$$

where  $\Sigma_{ij}^I(\phi)$  and  $\Sigma_{ij}^{II}(\phi)$  are universal functions describing the angular variation of the stress field, and  $K_I$  and  $K_{II}$  are the stress intensity factors (SIFs). The evolution of the crack tip is governed by the Griffith energy criterion (Griffith, 1920; Freund, 1990; Broberg, 1999; Leblond, 2003), which states that the intensity of the loading necessary to induce propagation is given by  $G = \Gamma$ , where  $G$  is the energy release rate and  $\Gamma$  is the fracture energy of the material, that is

the energy needed to create new free surfaces. This criterion can be rewritten using the stress intensity factor, in which case it is referred to as the Irwin criterion (Irwin, 1957)

$$K_I = K_{Ic} \equiv \sqrt{2\mu\Gamma}, \quad (2)$$

where  $K_{Ic}$  is the toughness of the material and  $\mu$  is the shear modulus. The Griffith criterion was originally formulated for quasi-static crack propagation (Griffith, 1920), and later generalized to rapidly moving cracks (Freund, 1990). While this criterion is very useful in predicting crack initiation, it cannot predict the direction of the crack tip, and therefore it is not sufficient to determine the actual path of the crack. In order to achieve this, several suggestions have been made. Among them, the Principle of Local Symmetry (PLS) states that the crack advances in such a way that in-plane shear stress vanishes in the vicinity of the crack tip, or explicitly

$$K_{II} = 0, \quad (3)$$

This rule was originally proposed for quasi-static cracks (Gol'dstein and Salganik, 1974; Leblond, 1989), and generalized to rapidly moving cracks (Adda-Bedia et al., 1999). Another suggestion, based on symmetry arguments, and which recovers the principle of local symmetry in a certain limit, was proposed by Hodgdon and Sethna (1993), who formulated an equation of motion of the crack tip. However, this formulation introduces additional length scales, which are not known *a priori*. A different approach, known as the maximum energy release rate criterion (Erdogan and Sih, 1963) states that the crack advances in a direction that maximizes its energy release rate. Interestingly, even though this approach is quite different from the PLS, it produces very similar results to those obtained using the PLS to such an extent that they were even conjectured to coincide (Bilby and Cardew, 1975). However, as shown in (Amestoy and Leblond, 1992) for kinked cracks and in (Katzav et al., 2007) for branched cracks, the results are not exactly the same and a clear distinction can be made between the two. Actually, it has been shown that the PLS is the only self-consistent criterion (Leblond, 1989, 2003).

Trying to address the problem of crack path prediction from the experimental side, the thermal crack problem has attracted a lot of attention. The propagation of cracks induced by thermal gradients has been widely studied (Ronsin et al., 1995; Ronsin, 1996; Yuse and Sano, 1997; Ronsin and Perrin, 1998; Yang and Ravi-Chandar, 2001; Deegan et al., 2003) since the work of Yuse and Sano (1993). In a typical experiment, a glass strip with a notch at its end is pulled at a constant velocity from an oven into a cold bath (see Fig. 1). The control parameters in this experiment are mainly the width of the strip, the temperature gradient between the oven and the cold bath, and the pulling velocity. If the velocity is small enough, a crack does not propagate. Above a first critical velocity, the crack starts propagating following a straight centered path, and above a second critical velocity, the crack begins to oscillate with a well defined wavelength. However, the nature of the transition from straight to wavy path is not fully understood. For example, the experimental results (Ronsin, 1996; Yuse and Sano, 1997) are not sufficient to determine whether the bifurcation is super-critical or sub-critical (also referred to as continuous or discontinuous transition)<sup>1</sup>. At higher pulling velocities, irregular oscillations and branching are observed. Interestingly, these are very reproducible regimes, which makes the thermal crack an ideal model experiment as it allows to study the slow propagation of cracks under well controlled conditions.

In an attempt to provide a theoretical explanation, Marder (1994) successfully determined the propagation threshold by calculating  $K_I$  for a straight crack propagating at the center of the

---

<sup>1</sup>In (Yuse and Sano, 1997), the bifurcation is claimed to be supercritical. Nonetheless, data points close to threshold are not accurate enough to rule out any other hypothesis (see Fig. 5 on page 372 in (Yuse and Sano, 1997)). Results presented in (Ronsin, 1996) suffer from the same lack of data points close to threshold.

plate. He also proposed a description of the oscillatory instability using the stability criterion derived by Cotterell and Rice (1980) for a crack in an infinite plate (the celebrated  $T$ -criterion), but that implied the improbable requirement that the fracture energy should depend strongly on the velocity. Eventually, this result was found to be incompatible with the experimental evidence (Ronsin et al., 1995), and serves as a classical example for the violation of the  $T$ -criterion. Sasa et al. (1994) attempted to predict the threshold of the oscillatory instability and its wavelength by using the PLS under the infinite-plate approximation. Although they gave a reasonable qualitative description, their results deviated systematically from the experimental measurements. The next step was taken by Adda-Bedia and Pomeau (1995), who calculated  $K_{II}$  directly for a sinusoidal perturbation in a finite strip, in the configuration where the crack tip is at the center of the strip. However, in order to predict the oscillatory instability they resorted to an additional criterion, namely that the stability with respect to this perturbation depends on the sign of  $K_{II}$ . More recently, Bouchbinder et al. (2003) wrote an amplitude equation for a sinusoidal perturbation using the propagation criterion of Hodgdon and Sethna (1993). One should note that all these approaches rely on additional criteria when determining the instability threshold and cannot do so using only the classical principles of crack propagation. In addition, theoretical results, except an attempt in (Bouchbinder et al., 2003), are mostly limited to the study of the linear stability of a straight crack or to the study of transient regimes. This situation calls for a reexamination of the thermal crack problem in order to explain it using solid arguments.

In this work, we begin with the study of quasistatic cracks in a quenched glass plate using a phase-field approach. Phase field models were originally introduced by Caginalp and Fife (1986); Collins and Levine (1986) to describe the propagation of solidification fronts. Extensions of this work allowed quantitative modeling of dendritic growth (Karma and Rappel, 1998) and since then, phase field methods have been applied to many solidification problems such as growth of binary alloys (Etchebarria et al., 2004) and formation of polycrystalline solids (Kobayashia and Warren, 2005). Furthermore, they have been extended to other free boundary problems including viscous fingering (Folch et al., 2000) and crack propagation (Karma et al., 2001; Karma and Lobkovsky, 2004; Henry and Levine, 2004; Hakim and Karma, 2005). It turns out that the numerical results of the phase-field model we derive are in quantitative agreement with experimental results of the actual system and allow to clarify the nature of the transition between straight and oscillatory cracks.

We then provide a theoretical analysis of the experiment of Yuse and Sano (1993). As in previous works (Adda-Bedia and Pomeau, 1995; Bouchbinder et al., 2003), the analysis is based on the calculation of the SIFs. However, we calculate them to first order with respect to a straight centered crack for an arbitrary trajectory in a strip of finite width. We are then able to determine the instability threshold and the wavelength of the oscillations using only the PLS without introducing any additional criterion. Results agree very well with the numerical simulations using the phase field model. And comparing them with the results of Adda-Bedia and Pomeau (1995), we find a small correction for the instability threshold, and a significant one for the wavelength. Also, unlike Bouchbinder et al. (2003), we argue that the calculation of the SIFs can be combined with the standard crack propagation criteria (that is with the Irwin criterion and the PLS) to obtain an evolution equation for the crack tip. Our main conclusion is that the PLS provides a good description of crack paths without any additional criteria.

The paper is organized as follows. We first provide a description of the thermal crack problem. We then describe the phase field approach for this problem, and compare its results with those of a theoretical analysis we perform. An important result of the theoretical analysis is an evolution equation for the crack path which allows quantitative predictions. We conclude by discussing the relevance of this work to path prediction of cracks in general.

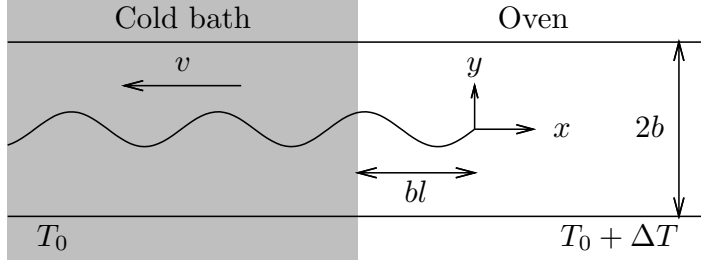


Figure 1: The experimental setup. A glass plate of width  $2b$  is moved slowly at a constant velocity  $v$  from an oven maintained at temperature  $T_0 + \Delta T$  to a cold bath of fixed temperature  $T_0$ . The crack tip is steady in the laboratory frame (moving in the plate frame) and its position with respect to the cold bath ( $bl$ ) is controlled by the temperature field.

## 2 The thermal crack problem

We first introduce the thermal crack problem and set the basic definitions and notations. Here, we consider the idealized problem of an infinitely long strip containing a semi-infinite crack. The coordinate system is chosen so that the axis of symmetry of the strip corresponds to  $y = 0$  and the tip of the crack lies at  $x = 0$  (see Fig. 1). We assume that the temperature field is uniform across the thickness of the strip, and that the strip is under plane stress conditions, so that the problem is actually two-dimensional. We will also use dimensionless variables, measuring the lengths in units of the half-width of the strip  $b$ , the temperature in units of  $\Delta T$ , the strains in units of  $\alpha_T \Delta T / b$ , and the stresses in units of  $E \alpha_T \Delta T$ , where  $E$  is the Young's modulus and  $\alpha_T$  the coefficient of thermal expansion. As will be shown, the behavior of the system is mainly governed by two dimensionless parameters : the Peclet number  $P = bv/D$ , where  $D$  is the thermal diffusion coefficient and the dimensionless material toughness  $\hat{K}_{Ic} = K_{Ic}/(E \alpha_T \Delta T \sqrt{b})$ .

Provided the velocity of the plate is not too low, the temperature field, which is assumed not to be affected by the presence of the crack, is well described by the advection-diffusion equation  $\partial_{xx}T + P\partial_xT = 0$ , with the boundary conditions:  $T(x) = 0$  in the cold bath and  $T(x) = 1$  for  $x \rightarrow \infty$  (Marder, 1994). The solution of this equation is

$$T(x) = \left(1 - e^{-P(x+l)}\right) \Theta(x+l) , \quad (4)$$

where  $x = -l$  corresponds to the location of the surface of the cold bath (see Fig. 1) and  $\Theta(x)$  is the Heaviside function.

We consider the problem of a crack propagating through the heated strip within the framework of linear elastic fracture mechanics. Under plane stress conditions, the two-dimensional stress tensor  $\bar{\sigma}$  is related to the two-dimensional strain tensor  $\bar{\epsilon}$  by

$$\sigma_{ij} = \frac{1}{1-\nu^2} [(1-\nu)\epsilon_{ij} + \nu\epsilon_{kk}\delta_{ij} - (1+\nu)T(x)\delta_{ij}] , \quad (5)$$

where  $\nu$  is the Poisson ratio and the strain tensor  $\bar{\epsilon}$  is related to the displacement field  $\vec{u}$  by

$$\epsilon_{ij} = \frac{1}{2} \left[ \frac{\partial u_i}{\partial x_j} + \frac{\partial u_j}{\partial x_i} \right] . \quad (6)$$

The strip is free from external traction, thus within any approach one should always satisfy the boundary conditions

$$\sigma_{yy}(x, \pm 1) = \sigma_{xy}(x, \pm 1) = 0 . \quad (7)$$

### 3 The phase field model

The classical theory of crack propagation, where the crack behavior is determined by the singularities of the stress field at the crack tip leads to difficult numerical issues when considering the movement and interaction of many cracks or to track crack motion in three dimensional systems where even the dynamics of crack fronts is not well understood. In this context, the phase field approach to crack propagation (Aranson et al., 2000; Karma et al., 2001; Eastgate et al., 2002; Marconi and Jagla, 2005) is very useful as it allows to study problems in arbitrary geometries and go beyond simple crack paths. It has succeeded in reproducing qualitative behavior of cracks such as branching (Karma and Lobkovsky, 2004) and oscillations under biaxial strain (Henry and Levine, 2004).

The general idea of phase field modeling is to introduce an additional field (the phase field) that describes the state of the system. The main advantage of this approach is that one does not need to treat the interface explicitly since it is defined implicitly as an isosurface of the phase field. This advantage becomes clear when studying the evolution of complex shapes since the algorithmic cost of using an additional field is much smaller than the cost of dealing explicitly with complex moving surfaces. In the case of fracture, this *phase field*  $\phi$  indicates whether the material is intact ( $\phi = 1$ ) or broken ( $\phi = 0$ ). In the usual sharp interface representation, a crack surface is an infinitely thin boundary between a region where the material is intact and an empty region that can not sustain any stress. In contrast, the equations of the phase field model are such that  $\phi$  varies continuously in space, and a crack surface is represented by a region of finite thickness. The thickness can be chosen freely and does not affect numerical results as long as it is much smaller than the characteristic length scale of the studied phenomenon. It can be shown that through an appropriate coupling between the phase field  $\phi$  and the elastic fields, the model can have the desired properties : no stresses are transmitted across a crack (in the limit where the system size is much larger than the width of the diffuse interface) and one can associate a finite surface energy with the interface, so that the fracture energy is well-defined.

Here, we use this model to describe a quasistatic crack propagating due to a thermal gradient. We begin by presenting the model, including the adjustments needed to incorporate thermoelastic effects. The dimensionless elastic energy is written as (Adda-Bedia and Pomeau, 1995)

$$E_{el} = \int \int dxdy g(\phi) \left[ \frac{1}{4(1-\nu)} (\epsilon_{kk} - 2T(x))^2 + \frac{1}{2(1+\nu)} \left( \epsilon_{ij} - \frac{\delta_{ij}}{2} \epsilon_{kk} \right)^2 \right], \quad (8)$$

where the function  $g(\phi) = \phi^3(4 - 3\phi)$  describes the coupling between the phase field and the elastic fields. This function is such that in regions where the material is broken ( $\phi = 0$ ), the contribution to the elastic energy is zero, while in regions where the material is intact, the contribution to the elastic energy recovers the one prescribed by linear elasticity. The particular choice of  $g$  is discussed in (Karma et al., 2001). The additional term  $T(x)$  corresponds to the thermal expansion. This effect is assumed to be the same in the intact and in the partially broken parts of the material.

Since we are considering a quasi-static crack growth, in which the elastic body is at mechanical equilibrium at all times, the elastic energy should be an extremum with respect to the displacement field  $\vec{u}(x, y)$ . That is

$$\frac{\delta E_{el}}{\delta u_i} = 0. \quad (9)$$

We now need to specify the evolution of the phase field. This is done by associating with the

phase field a dimensionless *free energy* given by (Henry and Levine, 2004)

$$E_\phi = \int \int dx dy \left[ \frac{D_\phi}{2} (\nabla \phi)^2 + V(\phi) + g(\phi) (\mathcal{E}_\phi - \mathcal{E}_c) \right], \quad (10)$$

where  $\mathcal{E}_\phi$  is defined by

$$\mathcal{E}_\phi = \begin{cases} \frac{1}{4(1-\nu)} (\epsilon_{kk} - 2T(x))^2 + \frac{1}{2(1+\nu)} \left( \epsilon_{ij} - \frac{\delta_{ij}}{2} \epsilon_{kk} \right)^2 & \text{if } (\epsilon_{ii} - 2T(x)) > 0 \\ \frac{1}{2(1+\nu)} \left( \epsilon_{ij} - \frac{\delta_{ij}}{2} \epsilon_{kk} \right)^2 & \text{if } (\epsilon_{ii} - 2T(x)) < 0 \end{cases}, \quad (11)$$

where  $V(\phi) = 1.5(1 - \phi^2)\phi^2$  is a double well potential that ensures that the preferred states of the homogeneous system are either  $\phi = 1$  (intact) or  $\phi = 0$  (completely broken).  $\mathcal{E}_\phi$  coincides with the standard elastic energy density when the material is under tension and includes only the contribution of shear when the material is under compression. This choice avoids the propagation of a crack under compression (Henry and Levine, 2004). Taking into account the coupling through  $g$  (which is such that  $g(1) = 1$ ,  $g(0) = g'(0) = g'(1) = 0$ ), when  $\mathcal{E}_\phi$  is larger than a threshold value  $\mathcal{E}_c$ , the broken phase is favored while when  $\mathcal{E}_\phi < \mathcal{E}_c$ , the intact phase is favored. The evolution equation for  $\phi$  is relaxational with a kinetic bias that ensures that the material will not be driven from a broken state to an intact state :

$$\tau \dot{\phi} = \min \left( -\frac{\delta E_\phi}{\delta \phi}, 0 \right), \quad (12)$$

where  $\tau$  is a constant. The irreversibility of Eq. (12) means that a crack cannot heal and ensures that the total elastic energy stored in the material cannot increase when  $\phi$  varies.

The elastic equation (9) is solved on a rectangular domain  $[-\frac{L}{2}, \frac{L}{2}] \times [-1, 1]$  with  $L \gg 1$  using the Gauss-Seidel over-relaxation method at each time step (Press et al., 2007). In addition to the boundary conditions (7), one has to set additional boundary conditions at  $x = \pm L/2$ . Here we have chosen

$$\epsilon_{ij}(-L/2, y) = 0, \quad (13)$$

$$\sigma_{xy}(L/2, y) = \sigma_{xx}(L/2, y) = 0. \quad (14)$$

It is clear that the final solution is insensitive to these boundary conditions as long as  $L \gg 1/P$ . The phase field equation (12) is solved using an Euler forward scheme (Press et al., 2007). The coefficient  $D_\phi = 4.4 \times 10^{-3}$  is chosen so that the diffuse interface has a thickness of few grid points, while  $\tau = 1$  is chosen so that the phase-field relaxes fast enough to its equilibrium (or more precisely, multiplying  $\tau$  by a factor 2 does not affect quantitatively the results.). Numerical checks were performed to ensure that neither changes in the convergence criterion of the Gauss-Seidel iterative method nor changes in the grid resolution affect the results significantly. The size of the domain  $[L] \times [2]$  was typically  $1500 \times 300$  grid points, and numerical checks showed that doubling  $L$  did not affect the results. Finally, the dimensionless fracture energy  $\hat{\Gamma} = \hat{K}_{Ic}^2$  was computed using the expression (Karma et al., 2001)

$$\hat{\Gamma} = \int_0^1 d\phi \sqrt{2D_\phi (\mathcal{E}_c - (\mathcal{E}_c g(\phi) - V(\phi)))}, \quad (15)$$

which is the actual value obtained during the numerical simulations, and using the expression  $\hat{\Gamma} = -dE_{el}/dx_c$  where  $x_c$  is the length of the crack and  $E_{el}$  is the elastic energy. This assumes that the crack under consideration is at equilibrium. These two approaches give the same value for the fracture energy within a relative error smaller than 10%.

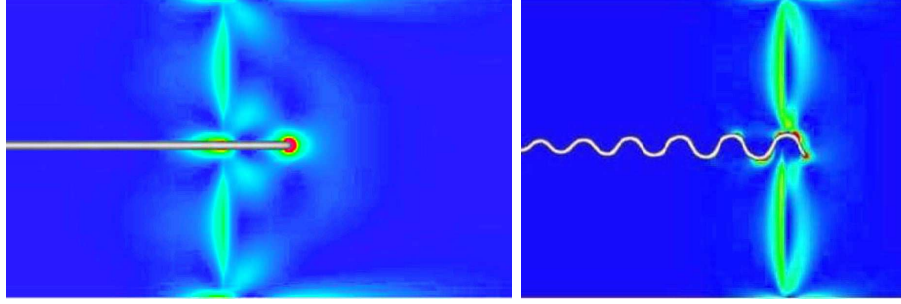


Figure 2: Typical crack paths obtained using the phase field model. The white region corresponds to the broken surface and the color code corresponds to the density of elastic energy in the material (red: high elastic energy density, blue: zero elastic energy). **(a)** A straight centered propagating crack. **(b)** A wavy crack above the instability threshold. This picture shows that the crack width is much smaller than the wavelength of the observed oscillations.

### 3.1 Numerical results

We now summarize the results of the simulations. By tuning the control parameters  $P$  and  $\hat{K}_{1c}$ , we could observe the different regimes observed in experiments : no crack propagation, propagation of a straight crack at the center of the strip or a crack following a wavy path (see Fig. 2). However, the main purpose of the present simulations was to determine the nature of the bifurcation from straight to oscillatory cracks, since no direct experimental results are available. Namely in experiments, the amplitude of oscillations varies almost linearly with the control parameter, but since experimental results do not allow to explore the behavior of the crack close to the threshold it was impossible to characterize the crack path in the close vicinity of the transition point. Furthermore, it should be emphasized that apart from attempts describing this transition by a Landau-Ginzburg expansion (Bahr et al., 1995; Bouchbinder et al., 2003), the available theoretical work has been mostly limited to linear stability analysis. Using the phase field model and without resorting to any assumption, we were able to compute the steady-state paths and to determine the nature of the bifurcation.

First, in Fig. 3 we present some typical crack paths close to the threshold for the sake of comparison with the analytical results presented below and also in order to clarify the nature of the bifurcation. The first path was obtained with an initial straight crack which was off center and below the threshold. One can see damped oscillations as the crack path returns to its equilibrium state: a straight crack. The second path was obtained with an initial crack that was *slightly* off center (shifted by 2 grid points away from the center) and *slightly* above the threshold. One can see oscillations of the path that are amplified as the crack advances. These oscillations eventually saturate and the crack path becomes oscillating with a finite constant amplitude as observed in experiments. Using the model we were able to compute the amplitude of the oscillations when a steady state was reached. Typical results are shown in Fig. 4 where the square of the amplitude is plotted as a function of  $1/\hat{K}_{1c}$  for a given value of  $P$ . One can see that above a threshold value of  $\hat{K}_{1c}$  the amplitude of oscillations is no longer zero and scales as the square root of the deviation from the threshold. The same behavior holds when using the value of  $P$  as a control parameter. The amplitude curves together with the damped oscillations below the threshold and the amplified oscillations above the threshold indicate that the bifurcation is supercritical or continuous.

For values of the control parameters well above the threshold, we were not able to recover complex paths similar to those observed in experiments (Yuse and Sano, 1993). This may

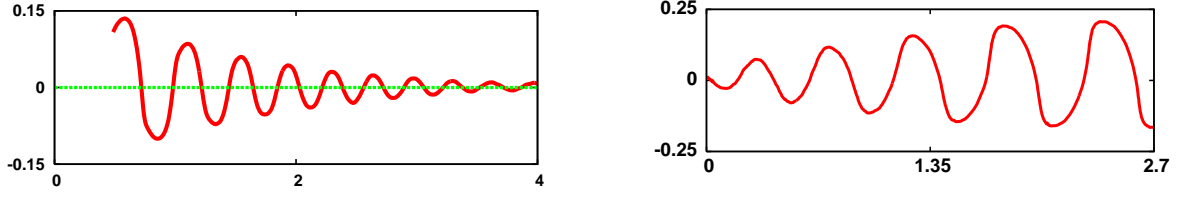


Figure 3: **(a)**: Crack tip trajectory below the threshold of linear instability for a crack which was initially off center.  $P = 7.9$  and  $1/\hat{K}_{\text{Ic}} = 7.85$ . **(b)**: Crack tip trajectory for an initially slightly off center crack above the threshold of linear instability.  $P = 7.9$  and  $1/\hat{K}_{\text{Ic}} = 8.43$ .

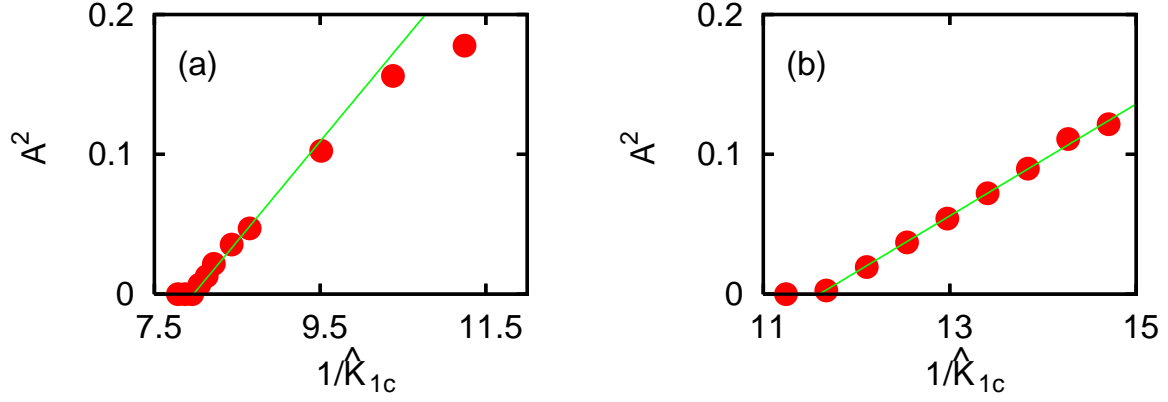


Figure 4: **(a)** Square of the amplitude  $A$  of the oscillations for  $P = 7.89$  as function of  $1/\hat{K}_{\text{Ic}}$ , which is related to the amplitude of the temperature gradient. **(b)**: same as **(a)** with  $P = 3.95$ . The linear behavior of  $A^2$  in the neighborhood of the transition shows that the transition from straight to oscillatory propagation is supercritical (continuous).

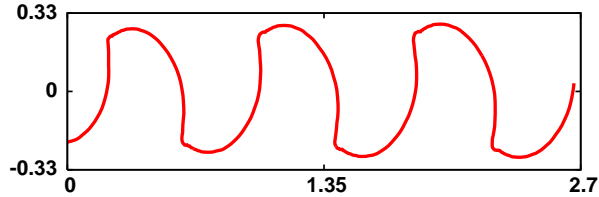


Figure 5: Crack tip trajectory for a crack deep in the nonlinear regime, that is far above the threshold of the instability. The values of the control parameters are  $P = 7.9$  and  $1/\hat{K}_{\text{Ic}} = 11.6$ . Note the striking resemblance to crack paths appearing in (Ghatak and Mahadevan, 2003; Audoly et al., 2005; Sendova and Willis, 2003).



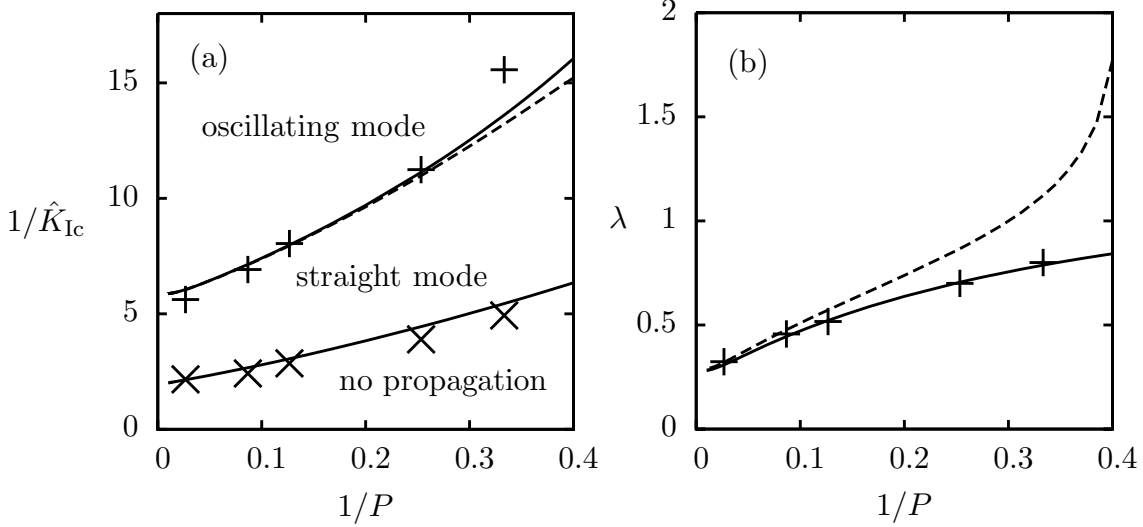


Figure 6: Main theoretical and numerical results. (a) The phase diagram of the different states of the system as a function of the two control parameters  $P$  and  $\hat{K}_{Ic}$ . (b) The wavelength  $\lambda$  as a function of  $P$  at the transition from straight to wavy crack propagation. In both figures, the symbols  $+$  and  $\times$  correspond to the numerical results obtained from the phase field model, the solid lines correspond to the analytical calculation presented in Sec. 4 and the dashed lines correspond to the results reported in (Adda-Bedia and Pomeau, 1995).

be due to the fact that well above the threshold the quasistatic approximation is no longer valid and dynamic effects through the temperature field as given by Eq. 4 become relevant. It is nonetheless interesting to note that the observed crescent-like path in Fig. 5 exhibits a striking similitude with paths obtained when cutting a thin elastic sheet with a moving thick object (Ghatak and Mahadevan, 2003; Audoly et al., 2005) and with crack paths obtained during drying of silicate sol-gel films fabricated using spin-coating techniques (Sendova and Willis, 2003).

The phase diagram in Fig. 6(a) shows the threshold for the propagation of a centered straight crack and for the transition to a wavy crack propagation in the  $1/P$ - $1/\hat{K}_{Ic}$  phase space. It can be seen that the theoretical predictions presented in Sec. 4 are in quantitative agreement with numerical results of the phase field model without any adjustable parameters. The same agreement is reached when considering the dimensionless wavelength at the threshold of the transition from straight to wavy crack path (see Fig. 6(b)). For this latter quantity, one should also note the good agreement with experimental values for small values of  $1/P$  (linear behavior with  $\lambda \simeq 0.28 + 2.0/P$ ) (Ronsin et al., 1995). Moreover, the phase field computation and our theoretical approach lead to the same deviation from the linear behavior for  $1/P > 0.2$ , where the discrepancy between the present results and those reported in (Adda-Bedia and Pomeau, 1995) become important. This feature has also been observed in experiments (Ronsin, 1996).

## 4 Theoretical analysis

We now turn to a theoretical study of the transition from straight to oscillatory crack propagation. As in previous theoretical treatments (Marder, 1994; Adda-Bedia and Pomeau, 1995; Bouchbinder et al., 2003), the analysis is based on the calculation of the stress intensity factors

(SIFs). However, here, they are computed to first order for an arbitrary trajectory without using the infinite plate approximation and without the restriction that the crack tip lies at the center of the sample. Within the framework of linear elastic fracture mechanics, the propagation of a crack is governed by the singular behavior of the stress field in the vicinity of its tip, as defined in Eq. (1). The propagation laws we use are the Irwin criterion defined in Eq. (2) and the principle of local symmetry (PLS) defined in Eq. (3). To calculate the SIFs, one must solve the equilibrium equations

$$\frac{\partial \sigma_{ij}}{\partial x_j} = 0, \quad \nabla^2 \sigma_{ii} = -\nabla^2 T(x), \quad (16)$$

with the boundary conditions (7) at the sides of the plate and the additional boundary condition at the crack surface

$$\sigma_{ij} n_j = 0, \quad (17)$$

where  $\vec{n}$  is the normal to the crack faces.

To investigate the transition from a straight to an oscillating regime, we consider a small deviation from a straight centered crack,

$$y(x) = Ah(x), \quad (18)$$

where  $h(x)$  is defined for  $x \leq 0$  (see Fig. 1) and  $|A| \ll 1$ . We expand the displacement and stress fields to first order as

$$u_i = u_i^{(0)} + Au_i^{(1)} + O(A^2), \quad (19)$$

$$\sigma_{ij} = \sigma_{ij}^{(0)} + A\sigma_{ij}^{(1)} + O(A^2). \quad (20)$$

The SIF  $K_I$  (resp.  $K_{II}$ ) is an even (resp. odd) function of  $A$ . Therefore their expansions have the form

$$K_I = K_I^{(0)} + O(A^2), \quad (21)$$

$$K_{II} = AK_{II}^{(1)} + O(A^3). \quad (22)$$

Note that in particular,  $K_{II} = 0$  for a straight centered crack. The different terms of the above expansion can be determined by solving the equilibrium equations using repeatedly the Wiener-Hopf method. The details of these calculations are presented in Appendix A. Here we simply summarize the calculation of  $K_{II}^{(1)}$ , which is novel.  $K_{II}^{(1)}$  can be written as

$$K_{II}^{(1)}[h(x)] = \kappa h(0) + K_{II}^{(1)}[h(x) - h(0)], \quad (23)$$

which amounts to decomposing the general problem into that of a straight off-center crack and that of an oscillating crack with a centered tip. The latter problem was solved by Adda-Bedia and Pomeau (1995), yielding

$$K_{II}^{(1)}[h(x) - h(0)] = \frac{K_I^{(0)}}{2} h'(0) + \int_{-\infty}^0 dx \frac{\partial}{\partial x} \left[ \sigma_{xx}^{(0)}(x, 0)(h(x) - h(0)) \right] p^+(-x), \quad (24)$$

where  $p^+(x)$  is a weight function that does not depend on the physical parameters. We have generalized the results of Adda-Bedia and Pomeau (1995) with the calculation of the contribution  $\kappa h(0)$  to obtain

$$K_{II}^{(1)}[h(x)] = \left[ cK_I^{(0)} - \frac{\partial}{\partial l} K_I^{(0)} \right] h(0) + \frac{K_I^{(0)}}{2} h'(0) + \int_{-\infty}^0 dx \frac{\partial}{\partial x} \left[ \sigma_{xx}^{(0)}(x, 0)h(x) \right] p^+(-x), \quad (25)$$

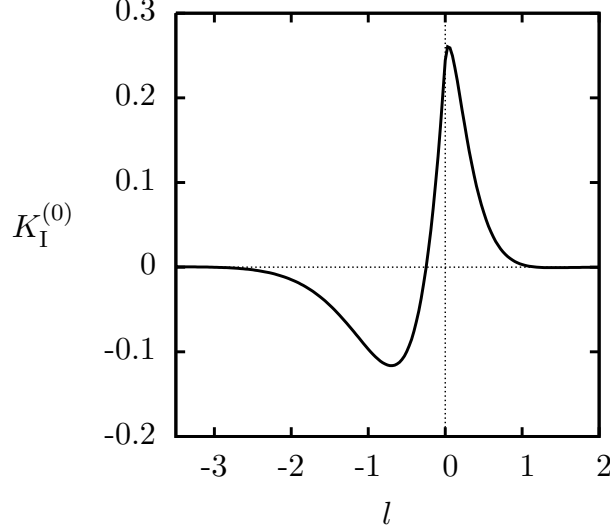


Figure 7:  $K_I^{(0)}$  as a function of  $l$ , for  $P = 5$ . Recall that  $l$  is the distance of the crack tip from the boundary of the cold bath. The threshold of incipient growth of a centered straight crack is given by  $\hat{K}_{\text{Ic}} = K_I^{(0)}(l_c)$ , where  $l_c$  is the location of the maximum of  $K_I^{(0)}(l)$ .

where  $c \simeq 1.272$  is a numerical constant (see Appendix A).

Having calculated the SIFs to first order, we can now examine the particular form taken by the crack propagation criteria for a small perturbation. The Irwin criterion reads  $K_I^{(0)} = \hat{K}_{\text{Ic}}$ . The transition to a propagating straight crack is thus governed by the existence of  $l$  such that  $K_I^{(0)}(l) = \hat{K}_{\text{Ic}}$ . This occurs when  $\hat{K}_{\text{Ic}} = K_I^{(0)}(l_c)$ , where  $l_c$  is the location of the maximum of  $K_I^{(0)}(l)$  (see Fig. 7). This condition determines the transition curve in Fig. 2 from no crack propagation to a propagation of a centered straight crack. Also, above the propagation threshold and to first order, Eq. (21) shows that the distance between the cold front and the crack tip does not depend on the crack path. This simplifies the problem, as we can parameterize the “time” evolution of the crack path by the position of its tip in a coordinate system attached to the plate. If  $h(x)$  now describes the crack path in such a coordinate system, the value of  $K_{\text{II}}^{(1)}$  when the tip is at the point  $x$  is simply given by

$$K_{\text{II}}^{(1)}(x) = \left[ cK_I^{(0)} - \frac{\partial}{\partial l} K_I^{(0)} \right] h(x) + \frac{K_I^{(0)}}{2} h'(x) + \int_{-\infty}^0 du \frac{\partial}{\partial u} \left[ \sigma_{xx}^{(0)}(u, 0) h(x + u) \right] p^+(-u) . \quad (26)$$

Therefore, the PLS which for a small perturbation reads  $K_{\text{II}}^{(1)}(x) = 0$ , yields

$$0 = \left[ cK_I^{(0)} - \frac{\partial}{\partial l} K_I^{(0)} \right] h(x) + \frac{K_I^{(0)}}{2} h'(x) + \int_{-\infty}^0 du \frac{\partial}{\partial u} \left[ \sigma_{xx}^{(0)}(u, 0) h(x + u) \right] p^+(-u) . \quad (27)$$

Eq. (27) is a linear equation for a crack that deviates slightly from the straight centered path.

#### 4.1 Oscillatory instability threshold

To determine the stability of the straight centered crack propagation, we must examine the evolution a small perturbation, which amounts to solving the following problem : given a crack path  $h(x)$  defined for  $x \leq 0$ , which does not necessarily satisfy  $K_{\text{II}}^{(1)}(x) = 0$  for  $x < 0$ , find a

continuation of  $h$  such that  $K_{\text{II}}^{(1)}(x) = 0$  for  $x > 0$ . Now, since  $\sigma_{xx}^{(0)}(x, 0)$  decreases exponentially as  $x \rightarrow -\infty$ , one can expect the long-term behavior of the crack to be the same as that of a crack path satisfying  $K_{\text{II}}^{(1)}(x) = 0$  for all  $x$ , and this is indeed observed in the simulations (see Fig. 3(b) in the previous section, and the discussion below). Accordingly, examining such crack paths suffices to determine the stability threshold.

We look for solutions of the form

$$h(x) = \text{Re} [\delta \exp(iqx)] , \quad (28)$$

where  $\text{Re}$  stands for the real part,  $\delta$  and  $q$  are in general complex numbers. Then using Eq. (26),  $K_{\text{II}}^{(1)}(x)$  takes the form

$$K_{\text{II}}^{(1)}(x) = \text{Re} [\delta K_{\text{II}}(q) \exp(iqx)] , \quad (29)$$

where

$$K_{\text{II}}(q) = \left[ cK_{\text{I}}^{(0)} - \frac{\partial}{\partial l} K_{\text{I}}^{(0)} \right] + iq \frac{K_{\text{I}}^{(0)}}{2} + \int_{-\infty}^0 du \frac{\partial}{\partial u} \left[ \sigma_{xx}^{(0)}(u, 0) e^{iqu} \right] p^+(-u) . \quad (30)$$

A solution  $K_{\text{II}}^{(1)}(x) = 0$  is obtained if  $K_{\text{II}}(q) = 0$ , which is the dispersion relation of the problem. Since  $q$  and  $K_{\text{II}}(q)$  are in general complex numbers, we can expect the equation  $K_{\text{II}}(q) = 0$  to admit a discrete set of solutions for a given set of the dimensionless parameters  $P$  and  $\hat{K}_{\text{Ic}}$ . By examining the behavior of  $K_{\text{II}}(q)$ , we find that the stability is determined by solutions corresponding to a pair of conjugate oscillating modes, which are shown on Fig. 8(a) for a given value of  $P$ . When  $\text{Im}(q) > 0$ , the perturbation (28) is damped which implies that the straight and centered crack propagation is stable. When  $\text{Im}(q) < 0$ , the perturbation is amplified, leading to a wavy crack propagation regime. Thus the instability threshold corresponds to  $\text{Im}(q) = 0$ , and is denoted by  $q \equiv q_c$ . Using this result, another way to determine the instability threshold is illustrated in Fig. 8(b). It consists in supposing from the beginning that  $q \equiv \omega$  is a real number<sup>2</sup> and in looking for the specific value of  $\omega = q_c$  for which  $\text{Im}[K_{\text{II}}(\omega)] = 0$  and  $\text{Re}[K_{\text{II}}(\omega)] = 0$  simultaneously.

By repeating the above computation for different values of  $P$  and  $\hat{K}_{\text{Ic}}$ , we obtain in Fig. 6(a) the phase diagram and in Fig. 6(b) the wavelength of the oscillations at the threshold, which is given by  $\lambda = 2\pi/q_c$ . These figures show that a good quantitative agreement is reached with the numerical results of the phase field model for both the wavy instability threshold and the wavelength at the transition.

Our results for the instability threshold differ from those of Adda-Bedia and Pomeau (1995), in which the threshold is determined by the existence of a real solution  $q_c$  such that  $K_{\text{II}}^{(1)}[\sin \omega x] = \frac{dK_{\text{II}}^{(1)}}{d\omega}[\sin \omega x] = 0$  for  $x = 0$  and the stability criterion is based on the sign of  $K_{\text{II}}^{(1)}[\sin \omega x]$ . In general, such a solution has no reason to satisfy  $K_{\text{II}}^{(1)}(x) = 0$  for  $x \neq 0$ . Indeed, the wavelengths predicted by these two criteria differ significantly, especially for small values of  $P$  (see Fig. 6(b)). The thresholds predicted also differ, but less notably (see Fig. 6(a)). As can be seen in Fig. 8(b), the deviations between the estimates of  $\hat{K}_{\text{Ic}}$  and  $\lambda$  obtained by the two methods are related to the vertical and horizontal distances between the minimum of  $\text{Im}(K_{\text{II}})$  and its intersection with  $\text{Re}(K_{\text{II}})$ , and the vertical distance scales as the square of the horizontal one.

---

<sup>2</sup>we use  $\omega$  instead of  $q$  in order to emphasize the fact that it is a real number

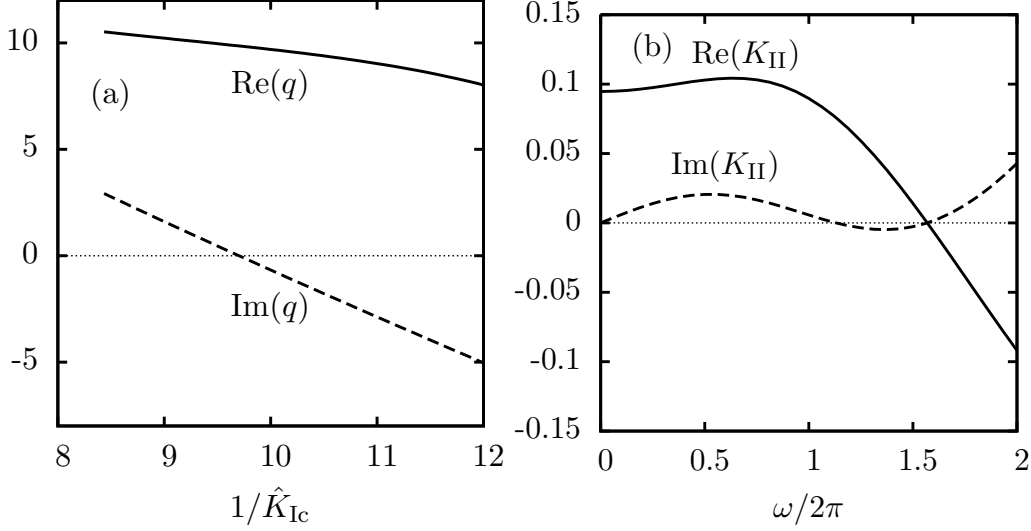


Figure 8: (a) Solutions of  $K_{\text{II}}(q) = 0$  versus  $1/\hat{K}_{\text{Ic}}$  for  $P = 5$ . The solution branch disappears when  $\text{Im}(q)$  exceeds a certain value, as the integral appearing in the calculation of  $K_{\text{II}}(q)$  ceases to converge. (b) The real and imaginary part of  $K_{\text{II}}(\omega)$ , with  $\omega$  real, at the instability threshold for  $P = 5$  ( $\hat{K}_{\text{Ic}} \simeq 0.103$ ).

## 5 An evolution equation for the crack path

In the previous section, we looked for smooth trajectories satisfying  $K_{\text{II}}^{(1)}(x) = 0$  for all  $x$ , which was sufficient to determine the instability threshold. We did not address the problem of the evolution of a crack path having an initial arbitrary shape  $h(x)$  for  $x \leq 0$ , which may also be of interest, and to which we now return. For this problem, equation (27) can be considered as an integro-differential equation for the crack profile  $h(x)$ . It resembles the equations obtained by Gol'dstein and Salganik (1974); Cotterell and Rice (1980) for cracks in an infinite plate. More specifically, it is a linear convolution equation, which can be solved formally using the Laplace transform, and numerically using a suitable scheme (see section 5.1 for a discussion).

We will first investigate the behavior of the solutions for small  $x$ . We show that the asymptotic expansion obtained by Amestoy and Leblond (1992) for cracks under remote loading with arbitrarily large kinks is also suited to the problem considered here. Using their notations, we consider an extension  $h^*$  of the crack path defined by

$$h^*(x) = \begin{cases} h(x) & \text{for } x \leq 0 \\ h(0) + xh'(0^-) + \theta x + ax^{3/2} + C/2x^2 & \text{for } x > 0 \end{cases} \quad (31)$$

Provided that the crack path is smooth enough (has a bounded curvature) for  $x < 0$ , it can be shown (see appendix B) that  $K_{\text{II}}^{(1)}$  along this extension satisfies

$$\begin{aligned} K_{\text{II}}^{(1)}[h^*, x] &= K_{\text{II}}^{(1)}(0^-) + \frac{K_{\text{I}}^{(0)}}{2}\theta + \frac{K_{\text{I}}^{(0)}}{2}(\alpha\theta + 3a/2)\sqrt{x} \\ &+ \left[ \kappa(h'(0^-) + \theta) + \int_{-\infty}^0 [h'(u) - h'(0)] g(u) du + \beta a + \frac{K_{\text{I}}^{(0)}}{2}C \right] x + O(x^{3/2}), \end{aligned} \quad (32)$$

where  $g(x) = \sigma_{xx}^{(0)}(x, 0)p^{+'}(-x)$ , and  $\alpha$  and  $\beta$  are constants that depend on  $l$ , the distance of the crack tip to the cold bath. A suitable choice of the unknown coefficients  $\theta$ ,  $a$  and  $C$  cancels all the terms of this expansion and thus the PLS is satisfied ( $K_{\text{II}}^{(1)}[h^*, x] = 0$ ). In the case of an

initial crack with  $K_{\text{II}}^{(1)}(0^-) = 0$ , one has  $\theta = 0$  and  $a = 0$  and thus the crack extension is regular at  $x = 0$ , i.e. there is no kink. As in the problem considered by Amestoy and Leblond (1992), Eq. (32) then reduces to an equation for the curvature  $C$ , which is related to the derivative of  $K_{\text{II}}^{(1)}$  along a straight extension:

$$K_{\text{II}}^{(1)}[h^*, x] = \frac{d}{dx} \left( K_{\text{II}}^{(1)}[h_{\text{straight}}^*, x] \right) x + \frac{K_{\text{I}}^{(0)}}{2} C x + O(x^{3/2}) , \quad (33)$$

where  $h_{\text{straight}}^*(x)$  is defined by

$$h_{\text{straight}}^*(x) = \begin{cases} h(x) & \text{for } x < 0 \\ h(0) + xh'(0^-) & \text{for } x \geq 0 \end{cases} . \quad (34)$$

Using the PLS, this implies the equation of motion

$$C = -\frac{2}{K_{\text{I}}^{(0)}} \frac{d}{dx} \left( K_{\text{II}}^{(1)}[h_{\text{straight}}^*, x] \right) . \quad (35)$$

## 5.1 Numerical crack path prediction

The results of the previous section can be used to discuss the numerical prediction of crack paths in the framework of linear elastic fracture mechanics. Strictly speaking, this discussion is relevant only to the solutions of the linear equation (27). However, the essential arguments in what follows are related to the regularity of crack paths. The most simple discretization of a crack path, and an often used one, is a semi-linear one, i.e. a series of straight segments of lengths  $\delta x$ . For each segment, equation (32) reduces to

$$\begin{aligned} K_{\text{II}}^{(1)}[h^*, x] &= K_{\text{II}}^{(1)}(0^-) + \frac{K_{\text{I}}^{(0)}}{2} \theta + \frac{K_{\text{I}}^{(0)}}{2} \alpha \theta \sqrt{x} \\ &+ \left[ \kappa(h'(0^-) + \theta) + \int_{-\infty}^0 [h'(u) - h'(0)] g(u) du \right] x + O(x^{3/2}) , \end{aligned} \quad (36)$$

From this equation, it can readily be seen that the typical accuracy (related to the residual value of  $K_{\text{II}}$  which deviates from  $K_{\text{II}} = 0$ ) along the segment is at best of order  $\delta x$ , which is rather poor. In our own simulations, we found that estimates of the instability threshold obtained from crack paths predicted using such a discretization are less accurate.

As an illustration, consider the scheme proposed by Bahr et al. (1995) (applied to a small perturbation, so that the above results hold). At each step, the temperature field is advanced by  $\delta x$  with the crack tip fixed (which amounts to replacing  $l$  by  $l - \delta x$ ), and the new values of the SIFs are computed. The crack tip must then advance by  $\delta x$  to satisfy again  $K_{\text{I}} = \hat{K}_{\text{Ic}}$ , and it is assumed to turn by  $\delta\theta = -2\delta K_{\text{II}}/K_{\text{I}}$ . However, if we use the expansion of the previous section (at a regular point), the different coefficients are of order  $a = O(\delta\theta) = O(\delta x)$  and  $C = O(1)$ , which yield contributions to the slope in  $x + \delta x$  of order  $\delta x^{3/2}$  (from  $a$ ) and  $\delta x$  (from  $C$ ). The former is negligible with respect to  $\delta\theta$ , but the latter is not.

Returning to the problem under consideration, provided that the path has a bounded curvature, an approximation by second order polynomials yields an inaccuracy of order  $\delta x^{3/2}$  (see below). Higher accuracy could theoretically be achieved using higher order polynomials for a sufficiently regular crack path, but it would make little sense to seek such an accuracy for a first-order perturbation equation, and such regularity cannot be expected in general. In fact, a typical crack path does not have a bounded curvature since it exhibits an initial kink, and approximation by polynomials will yield an accuracy of order  $\delta x^{1/2}$  whatever the order of the

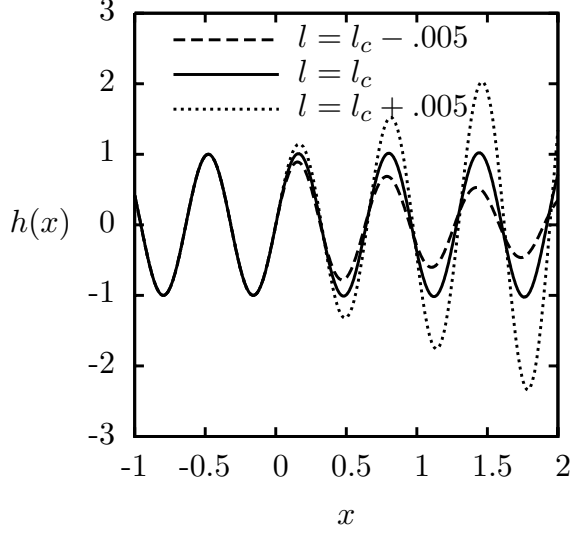


Figure 9: Crack paths near the predicted instability threshold for  $P = 5$  (solid line:  $l = l_c$  corresponding to  $\hat{K}_{Ic} \simeq 0.103$ ; dashed lines:  $l = l_c \pm .005$ ). The wavelength of the imposed initial oscillations ( $x \leq 0$ ) corresponds to the predicted wavelength of the spontaneous oscillations at the threshold.

polynomials. Sumi (1985) proposed using an expression of the form (31) for each segment. However, this form is appropriate only for the first step after a kink, and is not justified for subsequent steps. We propose, using the knowledge of the asymptotic behavior of the path near the kink at the origin the following: subtracting (for all  $x > 0$ ) the asymptotic behavior from the solution, a regular residual is obtained, which can be suitably approximated piecewise by second-order polynomials. This is a standard way to deal with the initial singularity of the solutions of Volterra equations. As we already suggested, nothing in this scheme depends on the specific loading considered (thermal loading) and on the fact that small perturbations are considered. Therefore, it seems that a similar scheme could be applied to other loading configurations and arbitrary crack paths.

In our simulations, which did not aim at a precise small-scale description of kinks, but rather at studying the large-scale behavior of crack paths, we did not implement the above scheme, and used an approximation by second-order polynomials. For a smooth path, the algorithm proceeds as follows: at each step, compute  $K_{II}^{(1)}(x + \delta x)$  for a straight extension from  $x$  to  $x + \delta x$ , then take the curvature

$$C = -\frac{2}{K_I^{(0)}} K_{II}^{(1)}(x + \delta x), \quad (37)$$

which cancels  $K_{II}^{(1)}(x + \delta x)$  to order  $\delta x^{3/2}$  according to equation (33), and replace the straight segment with the corresponding second-order polynomial. In that case, the deviations of  $K_{II}$  from 0 are of order  $\delta x^{3/2}$  everywhere along the resulting path. Now, the crack path is smooth only if  $K_{II}^{(1)} = 0$  at the starting point. Otherwise, we create a kink with the angle  $-2K_{II}^{(1)}/K_I^{(0)}$ , which cancels the initial shear component  $K_{II}^{(1)}$  right after the initial kink according to Eq. (32). The above error estimate no longer holds for the first few steps, but the large-scale behavior of the crack is not affected, since the influence of the initial kink decreases exponentially as the crack advances.

In Fig. 9 we show simulated crack paths near the instability threshold that confirm the results of section 4.1 by showing that an initial oscillatory perturbation with the predicted

wavelength preserves it wavelength, while its amplitude grows/remains the same/decays if the crack is above/at/below the threshold of the instability.

## 6 Conclusion

In this paper we address the problem of crack path prediction for quasi-static crack propagation. We used the framework of the thermal crack experiment since it is a well controlled experiment. The reason is that stresses are induced internally by an imposed thermal gradient that can be easily tuned by external parameters leading to a steady state propagation.

Our main result is that by using only the Principle of Local Symmetry and the Griffith criterion one can reproduce the phase diagram of the problem, namely predict the existence of the two instabilities (no-crack to straight crack and straight to oscillatory propagation). Furthermore, we show that these criteria are sufficient to determine the instability threshold and the wavelength of the oscillations without introducing additional hypotheses.

Another major achievement is the fact that we reproduce quantitatively the experimental results using a phase field model. This result allows to clarify the nature of the transition between straight and oscillatory cracks, which is convincingly shown to be supercritical or continuous. This is achieved thanks to the high resolution of the phase field approach near the transition point and the relative ease at which in-silico experiments can be performed under different conditions. This also suggests that the phase field model is more adapted than the classical methods for crack path tracking, especially when considering complex moving shapes, in view of its relatively low computational cost. It is therefore a good candidate to describe complicated crack patterns such as spirals or crescents as the ones observed in (Sendova and Willis, 2003), branching (Katzav et al., 2007) and interacting cracks (Marconi and Jagla, 2005). A real challenge for this approach would be to reproduce propagation of cracks in 3D, which can help to infer their laws of motion from such well controlled numerical experiments.

Interestingly, our theoretical results agree very well with the numerical simulations of the phase field model. This strengthens the theoretical approach based on the classical LEFM theory combined with the two propagation criteria, namely PLS and Griffith. This mostly validates of the Principle of Local Symmetry.

Last, we show that the calculation of the SIFs can be combined with the standard crack propagation criteria (that is with the Irwin criterion and the PLS) to obtain an evolution equation for the crack tip. This discussion shows that numerical crack path prediction is quite tricky, and that one has to be aware of the precision of the method used - which is closely related to the regularity properties of the crack paths under discussion. We argue that for crack paths that respect the PLS, and are therefore smooth, a piecewise second order polynomial approximation is the method of choice.

## Acknowledgements

This work was supported by the European Union MechPlant NEST project (F.C.) and by European Union PatForm Marie Curie action (E.K.). Laboratoire de Physique Statistique is associated with Universities Paris VI and Paris VII.



## A The straight off-center crack

In the following, we present briefly the method of resolution for a straight off-center crack in a thermal gradient. The method of resolution follows the same steps as in (Adda-Bedia and Pomeau, 1995). Consider a straight crack which is slightly above/below the center of the strip, namely its location is given by  $y(x) = Ah(0) \equiv \delta$ . Due to the absence of symmetry with respect to the center of the strip  $y = 0$ , let us split the displacement, strain and stress fields in the strip as follows

$$f(x, y) = \frac{1}{2} (f^+(x, y)\Theta(y - \delta) + f^-(x, y)\Theta(\delta - y)) , \quad (38)$$

where  $\Theta$  is the heaviside function and  $f$  stands for any component of the elastic fields. Let us also define

$$[f](x) = \frac{1}{2} (f^+(x, \delta) - f^-(x, \delta)) , \quad (39)$$

Note that all the elastic fields are continuous in the unbroken regions. However, along the crack surfaces the displacements might be discontinuous while  $\sigma_{yy}$  and  $\sigma_{xy}$  are continuous there. Thus, for this specific problem, the boundary conditions (7,17) can be rewritten as

$$\sigma_{yy}^\pm(x, \pm 1) = \sigma_{xy}^\pm(x, \pm 1) = 0 , \quad (40)$$

$$[\sigma_{yy}](x) = [\sigma_{xy}](x) = 0 , \quad (41)$$

$$[u_x](x) = [u_y](x) = 0 \quad \text{for } x > 0 , \quad (42)$$

$$\sigma_{yy}^\pm(x, \delta) = \sigma_{xy}^\pm(x, \delta) = 0 \quad \text{for } x < 0 , \quad (43)$$

Now, we Fourier transform along the  $x$  direction all the elastic fields and the temperature field and plug them into the equilibrium equations (16) and into the boundary conditions (40,41). After some algebraic manipulations, this yields relations of the type

$$\begin{pmatrix} [\hat{u}_x](k) \\ [\hat{u}_y](k) \end{pmatrix} = \begin{pmatrix} C_{xx}(k) & C_{xy}(k) & D_x(k) \\ C_{yx}(k) & C_{yy}(k) & D_y(k) \end{pmatrix} \begin{pmatrix} \hat{\sigma}_{xy}(k, \delta) \\ \hat{\sigma}_{yy}(k, \delta) \\ \hat{T}(k) \end{pmatrix} , \quad (44)$$

Performing the first-order expansions in  $\delta$ , as given by Eqs. (19)-(20):

$$\hat{u}_i(k, \delta) = \hat{u}_i^{(0)}(k, 0) + \delta \hat{u}_i^{(1)}(k, 0) , \quad (45)$$

$$\hat{\sigma}_{ij}(k, \delta) = \hat{\sigma}_{ij}^{(0)}(k, 0) + \delta \hat{\sigma}_{ij}^{(1)}(k, 0) , \quad (46)$$

and inverting (44) gives the final result

$$\hat{\sigma}_{yy}^{(0)}(k, 0) = -F(k) [\hat{u}_y^{(0)}](k, 0) + D(k) \hat{T}(k) , \quad (47)$$

$$\hat{\sigma}_{xx}^{(0)}(k, 0) = H(k) \hat{\sigma}_{yy}^{(0)}(k, 0) + S(k) \hat{T}(k) , \quad (48)$$

$$\hat{\sigma}_{xy}^{(1)}(k, 0) = -P(k) \left( [\hat{u}_x^{(1)}](k, 0) - ik [\hat{u}_y^{(0)}](k, 0) \right) + ik \hat{\sigma}_{xx}^{(0)}(k, 0) , \quad (49)$$

where

$$\begin{aligned} F(k) &= k \frac{\sinh^2 k - k^2}{\sinh 2k + 2k} , & D(k) &= 2 \frac{(1 - \cosh k)(\sinh k - k)}{\sinh 2k + 2k} , \\ H(k) &= \frac{k^2 + \sinh^2 k}{\sinh^2 k - k^2} , & S(k) &= \frac{\sinh k - k}{\sinh k + k} , \\ P(k) &= k \frac{\sinh^2 k - k^2}{\sinh 2k - 2k} . \end{aligned} \quad (50)$$

The first step of resolution which involves only the zeroth-order expansion, i.e. the case of a straight centered crack, is the calculation of  $K_I^{(0)}$ . Using the boundary conditions (42,43) to leading order and applying the Wiener-Hopf method to equation (47) yields (Adda-Bedia and Pomeau, 1995)

$$K_I^{(0)} = \int_{-\infty}^{+\infty} D(k) \hat{T}(k) F^+(k) \frac{dk}{2\pi}, \quad (51)$$

where

$$F(k) = \frac{F^-(k)}{F^+(k)}, \quad (52)$$

and  $F^+(k)$  ( $F^-(k)$ ) is analytic in the upper (lower) half-plane, respectively.

To complete the calculation of the SIFs, we return to the case of a straight off-center crack and determine the coefficient  $\kappa$  appearing in Eq. (23). Using the boundary conditions (42,43) to first order in  $\delta$  and applying again the Wiener-Hopf method to Eq. (49) yields

$$\begin{aligned} [\hat{u}_x^{(1)}](k) &= ik [\hat{u}_y^{(0)}](k) - \frac{1}{P^-(k)} \int_{-\infty}^{+\infty} \frac{ik' P^+(k') \hat{\sigma}_{xx}^{(0)-}(k', 0) dk'}{k' - k + i\epsilon} \frac{1}{2i\pi} + \frac{\alpha}{P^-(k)} \\ &= -\frac{k}{F^-(k)} \int_{-\infty}^{+\infty} \frac{D(k') \hat{T}(k') F^+(k') dk'}{k' - k + i\epsilon} \frac{1}{2\pi} \\ &\quad - \frac{1}{P^-(k)} \int_{-\infty}^{+\infty} \frac{ik' P^+(k') \hat{\sigma}_{xx}^{(0)-}(k', 0) dk'}{k' - k + i\epsilon} \frac{1}{2i\pi} + \frac{\alpha}{P^-(k)}, \end{aligned} \quad (53)$$

where  $P(k) = P^-(k)/P^+(k)$  with  $P^+(k)$  ( $P^-(k)$ ) analytic in the upper (lower) half-plane, and  $\epsilon$  is a vanishingly small positive number. notice that the solution of  $[\hat{u}_y^{(0)}](k)$  obtained from the zeroth order calculations has been used, and that  $\sigma_{xx}^{(0)}(x, 0)$  can be obtained from Eq. (48). For both  $F(k)$  and  $P(k)$  the factorization into  $F^\pm(k)$  and  $P^\pm(k)$  can be achieved using a Padé decomposition, as previously explained in (Bouchbinder et al., 2003; Katzav et al., 2007). The unknown constant  $\alpha$  is introduced because the decomposition involved in the Wiener-Hopf method is not unique. The value of  $\alpha$  can be determined by noting that the  $[\hat{u}_x^{(1)}](k)$  behaves as  $O(k^{-3/2})$  as  $k \rightarrow \infty$ . Canceling out the  $k^{-1/2}$  term on the r.h.s. yields

$$\alpha = - \int_{-\infty}^{+\infty} D(k) \hat{T}(k) F^+(k) \frac{dk}{2\pi}, \quad (54)$$

and thus one has

$$\begin{aligned} [\hat{u}_x^{(1)}](k) &= \left( \frac{1}{F^-(k)} - \frac{1}{P^-(k)} \right) \int_{-\infty}^{+\infty} D(k') \hat{T}(k') F^+(k') \frac{dk'}{2\pi} \\ &\quad + \frac{1}{F^-(k)} \int_{-\infty}^{+\infty} \frac{-ik' D(k') \hat{T}(k') F^+(k') dk'}{k' - k + i\epsilon} \frac{1}{2i\pi}. \end{aligned} \quad (55)$$

Finally by looking at asymptotic behavior of  $[\hat{u}_x^{(1)}](k)$  as  $k \rightarrow \infty$  one has

$$\kappa = c K_I^{(0)} - \frac{\partial}{\partial l} K_I^{(0)} - \int_{-\infty}^0 \frac{\partial}{\partial x} \sigma_{xx}^{(0)}(x, 0) p^+(-x) dx, \quad (56)$$

where  $p^+(x)$  is the inverse Fourier transform of  $P^+(k)$  and  $c$  is a numerical constant given by

$$c = \lim_{k \rightarrow \infty} \frac{(ik)^{\frac{3}{2}}}{\sqrt{2}} \left[ \frac{1}{F^-(k)} - \frac{1}{P^-(k)} \right] \simeq 1.272. \quad (57)$$

Using this value of  $\kappa$  in Eq. (23) yields Eq. (25).

## B The kinked and curved crack

We present here the derivation of Eq. (32). We begin by rewriting  $K_{\text{II}}^{(1)}(x)$  as

$$\begin{aligned}
K_{\text{II}}^{(1)}(x) &= \kappa h(x) + \frac{K_{\text{I}}^{(0)}}{2} h'(x) + \int_{-\infty}^0 dx \partial_u \left[ (h(x+u) - h(x)) \sigma_{xx}^{(0)}(u, 0) \right] p^{+}(-u) \\
&= \kappa h(x) + \frac{K_{\text{I}}^{(0)}}{2} h'(x) + \int_{-\infty}^0 dx [h(x+u) - h(x)] \sigma_{xx}^{(0)}(u, 0) p^{+}(-u) \\
&= \kappa h(x) + \frac{K_{\text{I}}^{(0)}}{2} h'(x) + I[h, x] ,
\end{aligned} \tag{58}$$

where

$$I[h, x] = \int_{-\infty}^0 [h(x+u) - h(x)] g(u) du , \tag{59}$$

and  $g(x) = \sigma_{xx}^{(0)}(x, 0) p^{+}(-x)$  behaves like  $x^{-3/2}$  when  $x \rightarrow 0$ . Let  $h(x)$  be a crack path defined for  $x \leq 0$  and having a bounded curvature, i.e. satisfying  $|h''(x)| < M$ . Defining

$$\epsilon(x, \delta x) = h(x + \delta x) - h(x) - h'(x) \delta x , \tag{60}$$

this implies

$$|\epsilon(x, \delta x)| < M(\delta x)^2/2 . \tag{61}$$

Using the definition of the straight extension given by Eq. (34) we obtain

$$\begin{aligned}
I[h_{\text{straight}}^*, x] &= \int_{-\infty}^0 [h^*(x+u) - h^*(x)] g(u) du \\
&= I[h, 0] + \int_{-\infty}^{-x} [h^*(x+u) - h(u) - h^*(x) + h(0)] g(u) du + \int_{-x}^0 [uh'(0) - h(u) + h(0)] g(u) du \\
&= I[h, 0] + x \int_{-\infty}^{-x} [h'(u) - h'(0)] g(u) du + \int_{-\infty}^{-x} [\epsilon(u, x) - \epsilon(0, x)] g(u) du - \int_{-x}^0 [\epsilon(0, u)] g(u) du \\
&= I[h, 0] + x \int_{-\infty}^0 [h'(u) - h'(0)] g(u) du + O(x^{3/2}) .
\end{aligned} \tag{62}$$

Defining the kinked and curved extension

$$h_{\text{kinked}}^*(x) = \begin{cases} h(x) & \text{for } x < 0 \\ h(0) + xh'(0) + \theta x + ax^{3/2} + C/2x^2 & \text{for } x > 0 \end{cases} , \tag{63}$$

we obtain

$$\begin{aligned}
I[h_{\text{kinked}}^*, x] &= I[h_{\text{straight}}^*, x] + \int_{-x}^0 \left[ \theta u + a \left( (x+u)^{3/2} - x^{3/2} \right) + C/2 \left( (x+u)^2 - x^2 \right) \right] g(u) du \\
&= I[h_{\text{straight}}^*, x] + \alpha \theta \sqrt{x} + \beta a x + O(x^{3/2}) ,
\end{aligned} \tag{64}$$

where  $\alpha$  and  $\beta$  are constants. Finally,

$$\begin{aligned}
K_{\text{II}}^{(1)}[h_{\text{kinked}}^*, x] &= K_{\text{II}}^{(0)}[h, 0^-] + \frac{K_{\text{I}}}{2} \theta + \frac{K_{\text{I}}}{2} (\alpha \theta + 3a/2) \sqrt{x} \\
&+ \left[ \kappa (h'(0) + \theta) + \int_{-\infty}^0 [h'(u) - h'(0)] g(u) du + \beta a + \frac{K_{\text{I}}}{2} C \right] x + O(x^{3/2})
\end{aligned} \tag{65}$$

## References

- Adda-Bedia M, Pomeau Y (1995) Crack instabilities of a heated glass strip. *Phys Rev E* 52:4105–4113
- Adda-Bedia M, Arias R, Ben Amar M, Lund F (1999b) Generalized Griffith criterion for dynamic fracture and the stability of crack motion at high velocities. *Phys Rev E* 60:2366–2376
- Amestoy M, Leblond JB (1992) Crack paths in plane situations–II. Detailed form of the expansion of the stress intensity factors. *Int J Solids Struct* 29:465–501
- Aranson IS, Kalatsky VA, Vonokur VM (2000) Continuum field description of crack propagation *Phys Rev Lett* 85:118–121
- Audoly B, Roman B, Reis R (2005) Cracks in brittle elastic plates: when geometry rules fracture paths. *Phys Rev Lett* 95:025502
- Bahr HA, Gerbatsch A, Bahr U, Weiss HJ (1995) Oscillatory instability in thermal cracking: a first-order phase-transition phenomenon. *Phys Rev E* 52:240–243
- Bilby BA, Cardew GE (1975) The crack with a kinked tip. *Int J Frac* 11:708–712
- Bouchbinder E, Hentschel HGE, Procaccia I (2003) Dynamical instabilities of quasistatic crack propagation under thermal stress. *Phys Rev E* 68:036601
- Broberg KB (1999) *Cracks and Fracture*. Academic Press, London
- Caginalp G, Fife P (1986) Phase Field Methods for Interfacial Boundaries *Phys Rev B* 33:7792–7794
- Collins JB, Levine H (1986) Diffuse interface model of diffusion-limited crystal growth *Phys Rev B* 31:6119–6122
- Cotterell B, Rice JR (1980) Slightly curved or kinked cracks. *Int J Fracture* 16:155–169
- Deegan RD, Chheda S, Patel L, Marder M, Swinney HL, Kim J, de Lozanne A (2003) Wavy and rough cracks in silicon. *Phys Rev E* 67:066209
- Eastgate LO, Sethna JP, Rauscher M, Cretegnny T, Chen CS, Myers CR (2002) Fracture in mode I using a conserved phase-field model. *Phys Rev E* 65:036117
- Erdogan G, Sih GC (1963) On the crack extension in plates under plane loading and transverse shear. *Journal of Basic Engineering* 85:519–527
- Etchebarria B, Folch R, Karma A, Plapp P (2004) Quantitative phase-field model of alloy solidification *Phys Rev E* 70:061604
- Fineberg J, Marder M (1999) Instability in dynamic fracture. *Phys Rep* 313:2–108
- Folch R, Casademunt J, Hernandez-Machado A (2000) Viscous fingering in liquid crystals: Anisotropy and morphological transitions *Phys Rev E* 61:6632–6638
- Freund LB (1990) *Dynamic Fracture Mechanics*. Cambridge University Press, Cambridge
- Ghatak A, Mahadevan L (2003) Crack street: the cycloidal wake of a cylinder ripping through a thin solid sheet. *Phys Rev Lett* 91:215507

- Gol'dstein RV, Salganik RL (1974) Brittle fracture of solids with arbitrary cracks. *Int J Fracture* 10:507–523
- Griffith AA (1920) The Phenomenon of Rupture and Flow in Solid. *Phil Trans R Soc Lond Ser A* *Int J Fracture* 221:163–198
- Hakim V, Karma A (2005) Crack path prediction in anisotropic brittle materials. *Phys Rev Lett* 95:235501
- Henry H, Levine H (2004) Dynamic instabilities of fracture under biaxial strain using a phase field model. *Phys Rev Lett* 93:105504
- Hodgdon JA, Sethna JP (1993) Derivation of a general three-dimensional crack-propagation law—A generalization of the principle of local symmetry. *Phys Rev B* 47:4831–4840
- Irwin GR (1957) Analysis of stresses and strains near the end of a crack traversing a plate. *J Appl Mech* 24:361–364
- Karma A, Rappel WJ (1998) Quantitative phase-field modeling of dendritic growth in two and three dimensions *Phys Rev E* 57:4323–4349
- Katzav E, Adda-Bedia M, Arias R (2007) Theory of dynamic crack branching in brittle materials. *Int J Fracture* 143:245–271
- Karma A, Kessler DA, Levine H (2001) Phase-field model of mode III dynamic fracture. *Phys Rev Lett* 87:045501
- Karma A, Lobkovsky AE (2004) Unsteady crack motion and branching in a phase field model of brittle fracture. *Phys Rev Lett* 92:245510
- Kobayashia R, Warren JA (2005) Modeling the formation and dynamics of polycrystals in 3D *Physica A* 356:127–132
- Leblond JB (1989) Crack paths in plane situations- I. General form of the expansion of the stress intensity factors. *Int J Solids Struct* 25:1311–1325
- Leblond JB (2003) *Mécanique de la rupture fragile et ductile*. Hermes Science Publications, Paris.
- Marconi VI, Jagla EA (2005) Diffuse interface approach to brittle fracture. *Phys Rev E* 71:036110
- Marder M (1994) Instability of a crack in a heated strip. *Phys Rev E* 49:51–54
- Press WH, Teukolsky SA, Vetterling WT, Flannery BP (2007) *Numerical Recipes*. Cambridge University Press, Cambridge
- Ronsin O, Heslot F, Perrin B (1995) Experimental study of quasistatic brittle crack propagation. *Phys Rev Lett* 75:2352–2355
- Ronsin O (1996) *Etude expérimentale de la propagation de fractures dirigées en milieu fragile*. PhD thesis, Université Paris VI
- Ronsin O, Perrin B (1998) Dynamics of quasistatic directional crack growth. *Phys Rev E* 58:7878–7886
- Sasa S, Sekimoto K, Nakanishi H (1994) Oscillatory instability of crack propagations in quasistatic fracture. *Phys Rev E* 50:1733–1736

- Sendova M, Willis K (2003) Spiral and curved periodic crack patterns in sol-gel films. *Appl Phys A* 76:957–959
- Sumi Y (1985) Computational crack path prediction. *Theoretical and applied fracture mechanics* 4:149–156
- Yang B, Ravi-Chandar K (2001) Crack path instabilities in a quenched glass plate. *J Mech Phys Solids* 49:91–130
- Yuse A, Sano M (1993) Transition between crack patterns in quenched glass plates. *Nature* 362:329–331
- Yuse A, Sano M (1997) Instabilities of quasi-static crack patterns in quenched glass plates. *Physica D* 108:365–378